SLAC-PUB-13529
February 2009

Omega3P: A Parallel Finite-Element Eigenmode Analysis Code for Accelerator Cavities

Lie-Quan Lee*, Zenghai Li, Cho Ng, and Kwok Ko
SLAC National Accelerator Laboratory, 2575 Sand Hill Road, Menlo Park, CA 94025

***Abstract*—Omega3P is a parallel eigenmode calculation code for accelerator cavities in frequency domain analysis using finite-element methods. In this report, we will present detailed finite-element formulations and resulting eigenvalue problems for lossless cavities, cavities with lossy materials, cavities with imperfectly conducting surfaces, and cavities with waveguide coupling. We will discuss the parallel algorithms for solving those eigenvalue problems and demonstrate modeling of accelerator cavities through different examples.**

Index Terms Accelerator cavities, finite element methods, frequency domain analysis, parallel algorithms.

I. Introduction

Frequency domain analysis is of a great importance in accelerator cavity design. Finite-element discretization can have high fidelity modeling for complex geometries of cavities. With parallel computing one can solve large-scale numerical problems that cannot be addressed in serial. We developed a parallel eigenmode calculation code for accelerator cavities in frequency domain analysis using finite-element methods. The report is organized as follows. In Section II, we formulate various eigenvalue problems for cavities with different properties. We discuss the algorithms used for solving those eigenvalue problems in Section III. We present parallelization strategy and software design in Section IV. We demonstrate Omega3P with 3 different examples in Section V. Finally, we summarized the report.

*Corresponding email: liequan@slac.stanford.edu

II. Frequency Domain Analysis for Acceleator Cavities

A. Vector Wave Equations

Maxwell s equations in differential form has three independent equations.

$$\nabla \times \overrightarrow{\mathbf{E}} = -\frac{\overrightarrow{\mathbf{B}}}{t} \quad (1)$$

$$\nabla \times \overrightarrow{\mathbf{H}} = \frac{\overrightarrow{\mathbf{D}}}{t} + \overrightarrow{\mathbf{J}} \quad (2)$$

$$\nabla \cdot \overrightarrow{\mathbf{D}} = \rho \quad (3)$$

For a simple medium, there are constitutive relations between field quantities.

$$\overrightarrow{\mathbf{D}} = {}_0 \overrightarrow{\mathbf{E}} \quad (4)$$

$$\overrightarrow{\mathbf{B}} = \mu_0 \mu \overrightarrow{\mathbf{H}} \quad (5)$$

where and μ are the relative electric permittivity and magnetic permeability while ${}_0$ and μ_0 are the values in the vacuum.

In analyzing eigenmodes of electromagnetic cavities, field quntities in Maxwell s equations can be written in the form of harmonically oscillating functions with a single frequency . Thus, the Maxwell s equations have a simplified form.

$$\nabla \times \overrightarrow{\mathbf{E}} = -j \overrightarrow{\mathbf{B}} \quad (6)$$

$$\nabla \times \overrightarrow{\mathbf{H}} = j \overrightarrow{\mathbf{D}} \quad (7)$$

By eliminating $\overrightarrow{\mathbf{B}}$ $\overrightarrow{\mathbf{H}}$ and $\overrightarrow{\mathbf{D}}$ or $\overrightarrow{\mathbf{E}}$ $\overrightarrow{\mathbf{B}}$ and $\overrightarrow{\mathbf{D}}$, one obtains

$$\nabla \times \left(\frac{1}{\mu} \nabla \times \overrightarrow{\mathbf{E}} \right) - k^2 \overrightarrow{\mathbf{E}} = 0 \quad (8)$$

$$\nabla \times \left(\frac{1}{} \nabla \times \overrightarrow{\mathbf{H}} \right) - \mu k^2 \overrightarrow{\mathbf{H}} = 0 \quad (9)$$

where k is the angular wavenumber $\frac{}{c}$ and c the speed of light. Either equation can be used in the numerical simulation. Eq (8) refers to E-formulation

Work supported in part by US Department of Energy contract DE-AC02-76SF00515

and Eq (9) H-formulation. Without loss of generality, we will use E-formulation for the rest of discussion.

In 1980, Nedelec discussed the construction of edge elements on tetrahedra and rectangular bricks [1]. Edge elements provide tangentially-continuous basis functions for discretizing electric field. The use of edge elements not only leads to convenient way of imposing boundary conditions at material interfaces as well as at conducting surfaces, but also treats conducting and dielectric edges and corners correctly. In Omega3P, a set of hierarchical high-order Nedelec basis functions [2] are used to discretize electric field.

$$\overrightarrow{\mathbf{E}} = \sum_i x_i \overrightarrow{\mathbf{N}}_i \tag{10}$$

B. Lossless Cavities

At a perfectly conducting surface, the boundary condition for electric field can be expressed as:

$$\overrightarrow{\mathbf{n}} \times \overrightarrow{\mathbf{E}} = 0 \tag{11}$$

where $\overrightarrow{\mathbf{n}}$ is the surface normal. If there is a symmetry in the cavity to be simulated, only a part of geometry needs to be modeled while the following boundary condition can be imposed on the symmetric plane.

$$\overrightarrow{\mathbf{n}} \times (\frac{1}{\mu}\nabla \times \overrightarrow{\mathbf{E}}) = 0 \tag{12}$$

where $\overrightarrow{\mathbf{n}}$ is the surface normal on the symmetric plane.

With finite element discretization in Eq (10), the vector wave equation (8) along with the boundary conditions (11) and (12) becomes a generalized eigenvalue problem for a lossless cavity:

$$\mathbf{K}\mathbf{x} = k^2\mathbf{M}\mathbf{x} \tag{13}$$

where the matrices $\mathbf{K}$ and $\mathbf{M}$ are

$$\mathbf{K}_{ij} = \left(\frac{1}{\mu}\nabla \times \overrightarrow{\mathbf{N}}_i \ \nabla \times \overrightarrow{\mathbf{N}}_j\right) \quad and \tag{14}$$

$$\mathbf{M}_{ij} = \left(\ \overrightarrow{\mathbf{N}}_i \ \overrightarrow{\mathbf{N}}_j\right) \tag{15}$$

Here we denote $(\overrightarrow{\mathbf{X}} \ \overrightarrow{\mathbf{Y}})$ to be an inner product, which is the integral over the domain $\int_\Omega \overrightarrow{\mathbf{X}} \cdot \overrightarrow{\mathbf{Y}}\, d\Omega$ and can be numerically evaluated with Gaussian integral rules. Note that matrix $\mathbf{M}$ is symmetric positive definite and matrix $\mathbf{K}$ is symmetric positive semi-definite with a large null space. Once the eigenvalue problem is solved, the electric field $\overrightarrow{\mathbf{E}}$ is recovered with Eq(10) while the magnetic field $\overrightarrow{\mathbf{B}}$ is computed with

$$\overrightarrow{\mathbf{B}} = -jkc\sum_i x_i \nabla \times \overrightarrow{\mathbf{N}}_i \tag{16}$$

where *j* is the square root of -1 and c the speed of light.

C. Cavities with Lossy Materials

The finite element analysis in the previous section can still be applied to cavities with lossy materials with the extension of using generalized variational principle [3]. In such cases, relative electric permittivity and/or magnetic permeability become complex in part or all of the domain. That makes mass matrix in Eq (14) and/or stiffness matrix in Eq (15) complex.

Note that the eigenvalue k also become complex. An physical quantity, quality factor, is defined as the real part of the eigenvalue divided by two times the imaginary part of the eigenvalue. Namely,

$$Q = \frac{k_{real}}{2k_{imag}} \tag{17}$$

The quality factor can be viewed as a measure of the loss. The high the Q value, the less the loss.

D. Cavities with Imperfectly Conducting Surfaces

When a cavity wall is an imperfect conductor, it can be shown that the electric and magnetic files at the surface of the conductor can be expressed as the following impedance boundary condition:

$$\overrightarrow{\mathbf{n}} \times (\frac{1}{\mu}\nabla \times \overrightarrow{\mathbf{E}}) - ik \ \ \overline{2\sigma}\overrightarrow{\mathbf{n}} \times (\overrightarrow{\mathbf{n}} \times \overrightarrow{\mathbf{E}}) = 0 \tag{18}$$

where σ is the electrical conductivity of the cavity wall. With the impedance boundary condition (18), the vector wave equation (8) can be descretized as a quadratic eigenvalue problem:

$$\mathbf{K}\mathbf{x} + ik\mathbf{W}\mathbf{x} = k^2\mathbf{M}\mathbf{x} \tag{19}$$

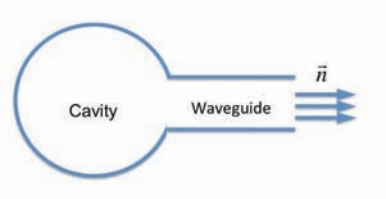

Fig. 1. A cavity connected with a waveguide. When the waveguide is long enough, the electric field inside the waveguide is a combination of the waveguide modes that can propagate.

E. Cavities with Waveguide Loading

An accelerating cavity is often connected with waveguides to input power or to damp the high-order modes. Fig 1 shows a cavity that is connected with a waveguide. When the waveguide is long enough, the electric field inside the waveguide can be expanded to a set of waveguide modes that can propagate inside the waveguide without attenuation. Therefore, as pointed in Ref [4], the boundary condition on the waveguide port can be expressed as follows:

$$\begin{aligned}\overrightarrow{\mathbf{n}} \times (\frac{1}{\mu}\nabla \times \overrightarrow{\mathbf{E}}) &- i\gamma_0 e_0^{TEM} \int_S e_0^{TEM} \cdot \overrightarrow{\mathbf{E}}\ dS \\ &- i\sum_m \gamma_m e_m^{TE} \int_S e_m^{TE} \cdot \overrightarrow{\mathbf{E}}\ dS \\ &+ i\sum_m \frac{k^2}{\gamma_m} e_m^{TM} \int_S e_m^{TM} \cdot \overrightarrow{\mathbf{E}}\ dS \\ &= 0 \end{aligned} \quad (20)$$

where $\gamma_m = \sqrt{k^2 - (k_m^c)^2}$ and k_m^c is the cut-off wavenumber of the mth waveguide mode. e_0^{TEM}, e_m^{TE}, and e_m^{TM} are the normalized waveguide TEM mode, mth TE mode, and mth TM mode, respectively.

The finite-element discretization of the vector wave equation (8) along with electric boundary condition (11), magnetic boundary condition (12) and waveguide boundary condtion (20) leads to a complex nonlinear eigenvalue problem (NEP):

$$\begin{aligned}\mathbf{Kx} &+ i\sqrt{k^2 - (k^c)^2}\mathbf{W^{TEM}x} \\ &+ i\sum_m \sqrt{k^2 - (k_m^c)^2}\mathbf{W_m^{TE}x} \\ &+ i\sum_m \frac{k^2}{\sqrt{k^2 - (k_m^c)^2}}\mathbf{W_m^{TM}x} \\ &= k^2\mathbf{Mx} \end{aligned} \quad (21)$$

where matrices $\mathbf{W^{TEM}}$, $\mathbf{W_m^{TE}}$, and $\mathbf{W_m^{TM}}$ are

$$\mathbf{W^{TEM}} = \int_S e_0^{TEM} \cdot \overrightarrow{\mathbf{N}}_i\ dS \int_S e_0^{TEM} \cdot \overrightarrow{\mathbf{N}}_j\ dS \quad (22)$$

$$\mathbf{W_m^{TE}} = \int_S e_m^{TE} \cdot \overrightarrow{\mathbf{N}}_i\ dS \int_S e_m^{TE} \cdot \overrightarrow{\mathbf{N}}_j\ dS \quad (23)$$

$$\mathbf{W_m^{TM}} = \int_S e_m^{TM} \cdot \overrightarrow{\mathbf{N}}_i\ dS \int_S e_m^{TM} \cdot \overrightarrow{\mathbf{N}}_j\ dS \quad (24)$$

Note that all the three types of matrices are symmetric but have dense blocks.

If the frequency of interest is above the first waveguide cutoff but below the second waveguide cutoff, i.e., only one waveguide mode can propagate in the waveguide, a simpler boundary condition can be used:

$$\overrightarrow{\mathbf{n}} \times (\frac{1}{\mu}\nabla \times \overrightarrow{\mathbf{E}}) - i\gamma \overrightarrow{\mathbf{n}} \times (\overrightarrow{\mathbf{n}} \times \overrightarrow{\mathbf{E}}) = 0 \quad (25)$$

where $\gamma = \sqrt{k^2 - (k^c)^2}$. We often refer (25) absorbing boundary condition (ABC). Note that ABC is accurate if there is only one waveguide mode propagating in the waveguide. Otherwise, it is just an approximation. With ABC, the discretized eigensystem becomes:

$$\mathbf{Kx} + i\sqrt{k^2 - (k^c)^2}\mathbf{Wx} = k^2\mathbf{Mx} \quad (26)$$

where matrix W is a sparse matrix and is defined as

$$\mathbf{W} = \int_{\mathbf{S}} (\overrightarrow{\mathbf{n}} \times \overrightarrow{\mathbf{Ni}}) \cdot (\overrightarrow{\mathbf{n}} \times \overrightarrow{\mathbf{N}}_{\mathbf{j}})\ \mathbf{dS} \quad (27)$$

III. Algorithms for Eigenvalue Problems

To solve eigenvalue problem (13), we use either the Implicit Restarted Arnoldi method through ARPACK [5] or an explicit restarted Arnodi method [6] implemented in Omega3P.

A shift-and-invert spectral transformation [7] is applied to Eq (13) in the process of solving the eigenvalue problems since the interior eigenvalues are of interest in the accelerator cavity modeling.

$$\frac{1}{k^2 - \sigma}\mathbf{x} = (\mathbf{K} - \sigma\mathbf{M})^{-1}\mathbf{Mx} \quad (28)$$

where σ is a prescribed shift close to the eigenvalues of interest. The above spectral transformation requires a solution of a highly indefinite linear system in every eigenvalue iteration, which is notoriously difficult to solve with iterative methods.

$$(\mathbf{K} - \sigma\mathbf{M})\,\mathbf{y} = \mathbf{Mb} \quad (29)$$

To solve the shifted linear system Eq(29), we often used sparse direct solvers [8], [9], [10] or Krylov subspace methods with multi-level preconditioners [11], [12], [13]. Sparse direct solvers require a large amount of memory to store the factor of the matrix $\mathbf{K} - \sigma\mathbf{M}$ thus their usage is limited.

The nonlinear eigenvalue problem (26) can be transformed into a quadratic eigenvalue problem by denoting $k = \sqrt{k^2 - (k^c)^2}$. We implemented the Second Order Arnoldi method [14] in Omega3P for solving the quadratic eigenvalue problem (19) and the nonlinear eigenvalue problem (26).

For solving the nonlinear eigenvalue problem (21), we implemented a self-consistent iteration [15], a nonlinear Jacobi-Davidson method [16], [17], and a nonlinear Rayleigh-Ritz iterative projection algorithm, NRRIT [18]. In the self-consistent iteration method, we first calculate an initial guess of an eigen-pair by ignoring all the waveguide terms in (21). That initial guess shall be a good approximation if the loss due to waveguide is not strong (quality factor is larger than 10). We use that to evaluate the waveguide terms and add them into the stiffness matrix and recalculate the eigen-pair. This loop terminates until the eigen-pair is self-consistent. It can be shown that the method will yield converged eigen-pairs as long as the loss is not strong.

IV. Parallelization Strategy and Software Design

Omega3P is written in C++ and uses MPI for inter process communication. It takes a tetrahedral mesh in NetCDF format as input for the geometry of the cavity. Domain decomposition is used for parallelization in Omega3P and the mesh is partitioned into P subdomains using ParMetis [19] or Zoltan [20] where P is the number of the MPI processors. A mesh region around process boundary is replicated in each processor to reduce communication. The hierarchical basis function described in [2] is employed for the discretization of the electric fields in the domain. The edge, face and volume degrees of freedom are located in parallel and matrices are assembled. After that, an appropriate eigensolver is invoked to find specific eigen-pairs, which are saved into files for further post-processing or for visualization purpose.

We use many 3rd party libraries in Omega3P and take a modular design as shown in Fig 2. For example, for linear algebra operations, we use the generic library described in [21]. That makes us very easy to add new solver components such as precondtioners for iterative linear solvers.

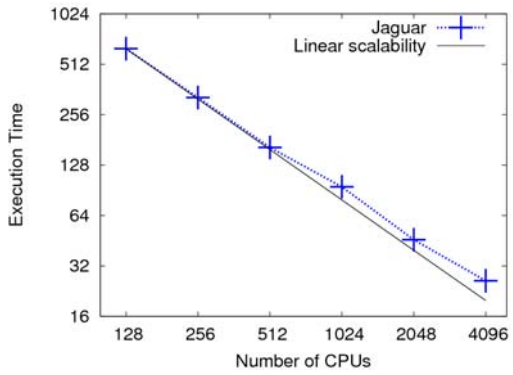

Fig. 3. The strong scalability of Omega3P on a Cray XT computer (Jaguar) at Oak Ridge National Laboratory.

Fig 3 shows the strong scalability of Omega3P running on a Cray XT computer with catamount kernel at Oak Ridge National Laboratory. The testing problem was for solving the π mode of the RF gun designed for the Linac Coherent Light Source. The computer model has 1.5 million tetrahedral elements. It resulted in a real eigenvalue problem with 9.6 million degrees of freedom and 506 million non-zero entries in the matrix of the eigen-system. As a comparison, the perfect linear scalability is also plotted as the black line. It is evident that Omega3P scales very well for this problem up to 4096 processors. In the case using 4096 processors, each processor on average has less than 400 tetrahedral elements.

V. Examples

A. A Spherical Cavity

In this example, we take a quarter of unit sphere cavity shown in Fig 4 and set all the three symmetric planes to be magnetic boundary. We generate a serial of quadratic tetrahedral meshes for a convergence study. We use Omega3P to compute the first 8 non-zero modes of this lossless cavity with 2nd order iso-parametic elements. The eigen-frequency results are listed in Table I.

B. A Damped Detuned Structure (DDS) Cell

In this example, we tested Omega3P with a cavity with imperfectly conducting surfaces shown Fig 5.

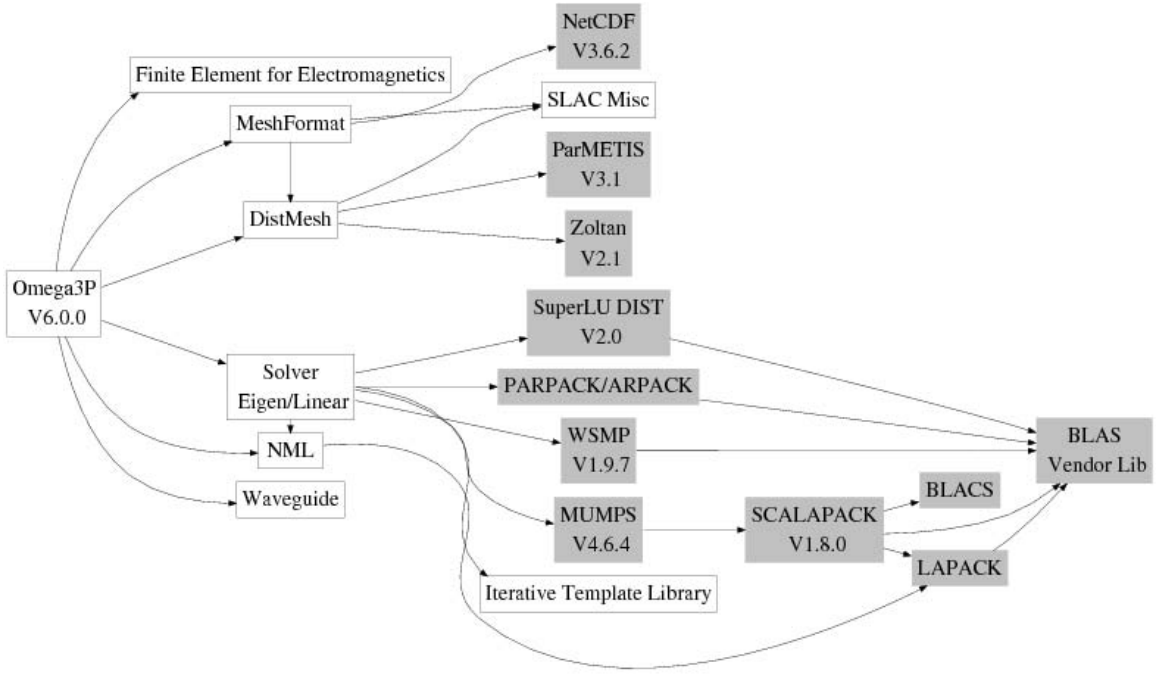

Fig. 2. The library dependency for Omega3P version 6. Grey boxes represent 3rd party libraries and white boxes are Omega3P internal libraries.

TABLE I

THE CONVERGENCE STUDY OF A QUARTER OF UNIT SPHERE. ALL THE THREE SYMMETRIC PLANES ARE SET TO BE MAGNETIC BOUNDARY. FOUR SET OF TETRAHEDRAL MESHES ARE GENERATED. MESH 1 HAS MESH SIZE OF 0.4 AND 76 ELEMENTS. MESH 2 HAS MESH SIZE OF 0.2 AND 494 ELEMENTS. MESH 3 HAS MESH SIZE OF 0.1 AND 4173 ELEMENTS. MESH 4 HAS MESH SIZE OF 30883 ELEMENT. MS STANDS FOR MESH SIZE. NE STANDS FOR THE NUMBER OF ELEMENTS. THE UNIT OF FREQUENCIES LISTED IS HZ.

Mode No.	Mesh 1 (MS=0.4, NE=76)	Mesh 2 (MS=0.2, NE=494)	Mesh 3 (MS=0.1 NE=4173)	Mesh 4 (MS=0.05, NE=30883)
0	184710699.0458458	184668561.5453410	184662807.1252133	184662469.1116296
1	184746123.6983275	184670011.8803936	184662831.0783886	184662470.1662160
2	289565891.0071810	289275483.5347070	289240006.0647894	289236779.6997921
3	289925940.4188058	289289885.9817063	289240233.4329534	289236802.7380072
4	290260435.5049497	289296420.3611495	289240375.0801812	289236806.8283637
5	333965112.5260288	333626751.6019411	333428670.6436561	333419095.1452913
6	355348302.7894213	355359797.5528432	355149284.9449404	355136370.7973798
7	355970365.9768929	355395570.6044523	355149826.1846064	355136415.2978936

The electrical conductivity of the copper surface is 5.8×10^7. We use a mesh with 19788 quadratic tetrahedral elements and second order basis functions. We compute both wall loss quality factor for a cavity with perfectly conducting surfaces and the quality factor from Eq (17) for a cavity with impedance boundary condition (18). The results from the former has been validated by microwave QC of the fabricated cells showing measured frequencies within 0.01% of target value [22], [23]. Table II lists the results of the frequencies and quality factors computed from both ways. They are in good agreement.

TABLE II

FREQUENCIES AND QUALITY FACTORS COMPUTED FOR A DDS CELL.

Method	Frequency	Quality Factor
Lossless cavity	11.4459 GHz	6523
Cavity with impedance BC	11.4468 GHz	6564

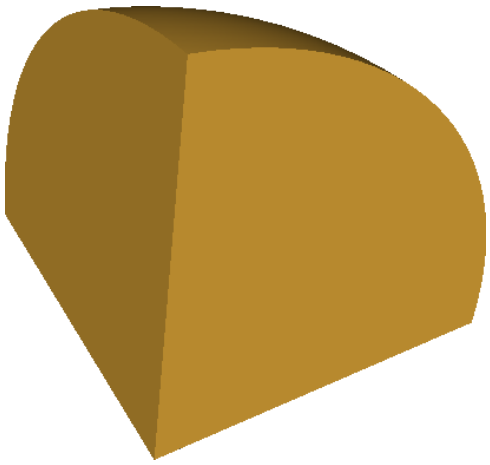

Fig. 4. A computer model for a quarter of spherical cavity.

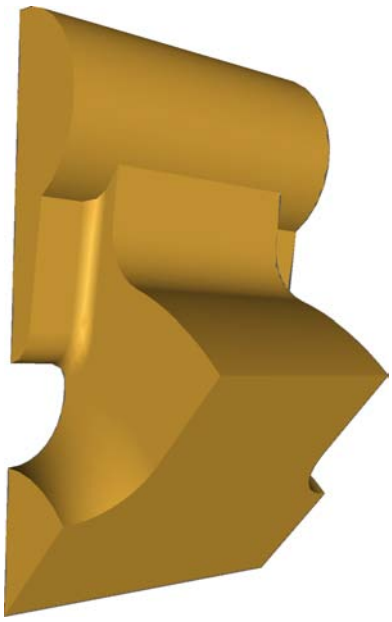

Fig. 5. A computer model for one eighth of the vacuum part of a DDS cell.

C. A Cavity Coupled with Rectangular Waveguides

Fig 6 shows a computer model of a cavity coupled with two identical rectangular waveguides. The first waveguide cutoff is 5.2597GHz. The frequency of the mode is around 9.4GHz, which is above the first cutoff but below the second cutoff. Thus, we can solve the eigenvalue problem (26) to compute the frequency and the quality factor of the mode. With a mesh of 8378 elements for a quarter geometry, the computed frequency is 9.3992GHz and the quality factor 177.98. Alternatively, we can use S-paramter calculations to decide resonance frequency and the quality factor by fitting the transmission coefficients in order to verify the results of the eigenvalue

Fig. 6. A computer model for a cavity coupled with two identical rectangular waveguides.

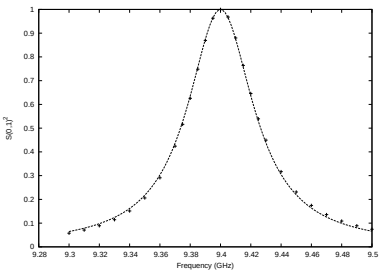

Fig. 7. Transmission coefficients versus operating frequencies in S parameter calculations for the cavity coupled with rectangular waveguides. The fitting curve is also plotted. The fitting function for $S(0,1)^2$ is $\frac{1}{1+Q^2(\frac{f}{f_0}-\frac{f_0}{f})^2}$. The fitted quality factor Q is 177.81 and resonance frequency 9.40 GHz.

computations. We used a mesh with 19818 elements for a half geometry in the S-parameter calculations. Fig 7 shows transmission coefficients with respect to operating frequencies in the cavity. We fitted the data and got the resonance frequency 9.40GHz and the quality factor 177.81, in remarkable agreement with those from eigenvalue computations.

VI. Summaries

We presented Omega3P, a parallel eigenmode calculation code for accelerator cavities in frequency domain analysis using finite-element methods. We described the detailed finite-element formulations and resulting eigenvalue problems for lossless cavities, cavities with lossy materials, cavities with imperfectly conducting surfaces, and cavities with waveguide coupling. We discussed the parallel algorithms for solving those eigenvalue problems

and demonstrated modeling of accelerator cavities through different examples.

ACKNOWLEDGMENT

This work is supported by the U.S. Department of Energy under contract number DE-AC02 -76SF00515. Part of the work used resources of the National Center for Computational Sciences at Oak Ridge National Laboratory and resources of the National Energy Research Scientific Computing Center, which are supported by the Office of Science of the Department of Energy under Contract DE-AC05-00OR22725 and DE-AC02-05CH11231, respectively.

REFERENCES

[1] J. C. Nedelec, "Mixed finite elements in r_3," *Numer. Metho.*, vol. 35, pp. 315–341, 1980.

[2] D.-K. Sun, J.-F. Lee, and Z. Cendes, "Construction of nearly orthogonal nedelec bases for rapid convergence with multilevel preconditioned solvers," *SIAM J. SCI. COMPUT*, vol. 23, no. 4, pp. 1053–1076, 2001.

[3] J. Jin, *The Finite Element Method in Electromangetics*, second edition ed. John Wiley & Sons, INC, 2002.

[4] Z. Lou and J. Jin, "An accurate waveguide port boundary condition for the time-domain finite-element method," *IEEE Antennas and Propagation Society International Symposium*, vol. 1B, pp. 117–120, 2005.

[5] R. B. Lehoucq, D. C. Sorensen, and C. Yang, *ARPACK Users Guide: Solution of Large Scale Eigenvalue Problems with Implicitly Restarted Arnoldi Methods*. SIAM, 1997.

[6] R. B. Morgan, "On restarting the arnoldi method for large nonsymmetric eigenvalue problems," *Mathematics of Computation*, vol. 65, no. 215, pp. 1213–1230, 1996.

[7] Z. Bai, J. Demmel, J. Dongarra, A. Ruhe, and H. van der Vorst, Eds., *Templates for the solution of Algebraic Eigenvalue Problems: A Practical Guide*. Philadelphia: SIAM, 2000.

[8] A. Gupta, G. Karypis, and V. Kumar, "A highly scalable parallel algorithm for sparse matrix factorization," *IEEE Transactions on Parallel and Distributed Systems*, vol. 8, no. 5, pp. 502–520, May 1997.

[9] P. Amestoy, I. Duff, J.-Y. LÉxcellent, and J. Koster, "A fully asynchronous multifrontal solver using distributed dynamic scheduling," *SIAM Journal on Matrix Analysis and Applications*, vol. 23, no. 1, pp. 15–41, 2001.

[10] X. S. Li and J. W. Demmel, "SuperLU_DIST: A scalable distributed-memory sparse direct solver for unsymmetric linear systems," *ACM Trans. Mathematical Software*, vol. 29, no. 2, pp. 110–140, June 2003.

[11] L.-Q. Lee, L. Ge, M. Kowalski, Z. Li, C.-K. Ng, G. Schussman, M. Wolf, and K. Ko, "Solving large sparse linear systems in end-to-end accelerator structure simulations," in *Proceedings of the 18th International Parallel and Distributed Processing Symposium*, Santa Fe, New Mexico, April 2004.

[12] L.-Q. Lee and et al, "Enabling technologies for petascale electromagnetic accelerator simulation," *J. Phys.: Conf. Ser.*, vol. 78, p. 012040, 2007.

[13] ——, "Computational science research in support of petascale electromagnetic modeling," in *Proceedings of SciDAC 2008 Conference*, Seattle, Washington, 2008.

[14] Z. Bai and Y. Su, "Soar: A second-order arnoldi method for the solution of the quadratic eigenvalue problem," *SIAM J. MATRIX ANAL. APPL.*, vol. 26, no. 3, pp. 640–659, 2005.

[15] L.-Q. Lee, L. Ge, Z. Li, C. Ng, K. Ko, B. shan Liao, Z. Bai, W. Gao, C. Y. an Parry Husbands, and E. Ng, "Solving nonlinear eigenvalue problems in accelerator cavity design," in *SIAM Annual Meeting*, 2005.

[16] T. Betcke and H. Voss, "A jacobi-davidson-type projection method for nonlinear eigenvalue problems," *Future Gener. Comput. Syst.*, vol. 20, no. 3, pp. 363–372, 2004.

[17] L.-Q. Lee, V. Akcelik, S. Chen, L. Ge, E. Prudencio, Z. Li, C. Ng, L. Xiao, and K. Ko, "Advancing computational science research for accelerator design and optimization," in *Proc. of SciDAC 2006 Conference*, Denver, Colorado, USA, June 2006.

[18] B.-S. Liao, Z. Bai, L.-Q. Lee, and K. Ko, "Solving large scale nonlinear eigenvalue problem in next-generation accelerator design," Stanford Linear Accelerator Center (SLAC), Tech. Rep. SLAC-PUB-12137, 2006.

[19] G. Karypis and V. Kumar, "Parallel multilevel k-way partitioning scheme for irregular graphs," *SIAM Review*, vol. 41, no. 2, pp. 278–300, 1999.

[20] K. Devine, E. Boman, R. Heaphy, B. Hendrickson, and C. Vaughan, "Zoltan data management services for parallel dynamic applications," *Computing in Science and Engineering*, vol. 4, no. 2, pp. 90–97, 2002.

[21] L.-Q. Lee and A. Lumsdaine, "Generic programming for high performance scientific applications," *Concurrency and Computation: Practice and Experience*, vol. 17, pp. 941–965, 2005.

[22] Z. Li and et al, "High-performance computing in accelerating structure design and analysis," *Nuclear Instruments and Methods in Physics Research Section A: Accelerators, Spectrometers, Detectors and Associated Equipment*, vol. 558, no. 1, pp. 168–174, 2005.

[23] ——, "X-band linear collider r&d in accelerating structures through advanced computing," in *Proceedings of EPAC 2004*, Lucerne, Switzerland, 2004.